

Robust and Scalable V2V Safety Communication Based on the SAE J2945/1 Standard

S M Osman Gani^{ID}, Member, IEEE, Yaser P. Fallah, and Hariharan Krishnan

Abstract—This article analyzes the scheduling protocol for basic safety messages standardized in the SAE J2945/1 and presents large-scale scalability results obtained from a high-fidelity simulation platform. The presented results demonstrate the protocol’s efficacy to address the scalability issues in vehicle-to-vehicle communication. By employing a distributed opportunistic approach, the SAE J2945/1 congestion control algorithm keeps the overall offered channel load within an optimal operating range, while meeting the minimum tracking requirements set forth by upper-layer applications. The scheduling protocol allows transmission of event-triggered and vehicle-dynamics driven messages that further the situational awareness in cooperative vehicle-to-vehicle communications. The validation results are evaluated using position tracking error as the main performance measure, with age of communicated information as the supporting evaluation measure of the congestion control algorithm. In addition, we examine the optimality of the default settings of the SAE J2915/1 congestion control algorithm parameters. Comprehensive analysis and trade-off study of the control parameters reveal some areas of improvement to further the algorithm’s efficacy.

Index Terms—Channel congestion control, information dissemination rate, CSMA/CA wireless networks, DSRC, V2V communication.

I. INTRODUCTION

SCALABLE communication is crucial in the realm of cooperative vehicle safety applications that are heavily dependent on the timely exchange of vehicle status updates in the form of basic safety messages (BSMs). Regardless of the underlying technology, a scalable communication protocol needs to be in place to optimize the safety benefits of vehicle-to-vehicle (V2V) applications. Such scalability mechanism is required to keep the interference level to a minimum, enabling timely dissemination and reception of critical BSMs. While a number of transmit parameters can be adapted to scale the capability of effective communication, BSM inter-transmit interval and transmit power prove to be the most viable options. A solution utilizing both of these control parameters to regulate the offered channel load is standardized in the

Manuscript received May 4, 2019; revised January 27, 2020 and July 13, 2020; accepted July 30, 2020. This work was supported in part by the National Science Foundation under CAREER Grant 1664968. The Associate Editor for this article was J. E. Narango. (*Corresponding author: S M Osman Gani*.)

S M Osman Gani and Yaser P. Fallah are with the Department of Electrical and Computer Engineering, University of Central Florida, Orlando, FL 32816 USA (e-mail: smosman.gani@knights.ucf.edu; yaser.fallah@ucf.edu).

Hariharan Krishnan is with the Electrical and Control Systems Research Laboratory, General Motors Global Research and Development Center, Warren, MI 48092 USA (e-mail: hariharan.krishnan@gm.com).

Digital Object Identifier 10.1109/TITS.2020.3016307

SAE International (SAE) J2945/1 [1] – a V2V communication protocol standardized only for light-duty vehicles to exchange information required for tracking remote vehicles. The BSM scheduling algorithm in the SAE J2945/1 is based on [2], [3]. The algorithm outlines an adaptive upper layer message rate control as a function of vehicle dynamics and estimated tracking error. The algorithm also adopts a transmit power control approach, as outlined in the SUPRA algorithm [4], as a function of the instantaneous channel busy percentage. Performance evaluation of the SAE J2945/1 congestion control (CC) algorithm is the main focus of this article, aiming at demonstrating its effectiveness in a busy multi-lane freeway and in a typical suburban 4-way intersection with varying traffic densities. This article also provides additional analysis to further the efficacy of the algorithm, in light of an extensive trade-off study of the chosen values for key congestion control parameters.

A. Related Work

In cooperative V2V communication system, channel congestion control mechanisms are desirably independent of the physical layer. However, the feedback measures used in such mechanisms have some intrinsic coupling with lower layers of the protocol stack. This article focuses on the channel congestion control of the IEEE 802.11p [5] based V2V communications operating in the Dedicated Short Range Communications (DSRC) band. In DSRC, channel congestion can be managed by adapting a number of transmit parameters, e.g., message length, inter-transmit time (ITT), transmit power, and data rate. Prior to the standardization of SAE J2945/1, BSM scheduling in V2V communication was considered to have a default fixed-rate fixed-power transmit policy for the envisioned cooperative vehicle safety systems. The scalability issue of such a flat message rate and transmit power based approach have been demonstrated by several works as reported in [3], [6]. To scale the V2V communication, many congestion control algorithms have been proposed in the literature that shows substantial scalability gain by adapting various transmit parameters (at the application and/or medium access control layers) jointly or separately. A detailed survey of the congestion control algorithms that are available in the existing literature is presented in [7]. In the next two subsections, we summarized some of the message scheduling mechanisms proposed in the existing literature by broadly classifying those into two groups – message rate and transmit power based approaches, and medium access control based approaches.

1) Message Rate and Transmit Power Based Congestion Control: In [2], the authors proposed a scalable communication method where each participating vehicle in the cooperative communication adjusts its BSM generation rate depending on the estimated tracking error as perceived by its neighboring vehicles. The sender vehicle also adapts the transmit power based on the observed channel load to further mitigate the channel congestion level by effectively limiting the range of communication and thus, limiting the effective interference range. Transmit power control is proposed to have a linear adjustment to keep the channel busy percentage (CBP) bounded within a minimum and a maximum value. The outlined algorithm also prioritizes BSM transmissions due to vehicle dynamics to ensure situational awareness to the neighboring vehicles. In [8], the authors provided a transmit power based congestion control algorithm that separately targets two different groups of vehicles, using two different transmit powers. The idea is to transmit high power packets for farther vehicles as well as for the nearby vehicles, while the low power transmits are only targeted for nearby ones. In [9], another CC mechanism called Linear Message Rate Integrated Control (LIMERIC), which is based on a linear message rate adaptation, has been outlined that makes the CBP to converge to the desired operating level as found in [3]. In [10], the authors enhanced the LIMERIC algorithm to adapt the transmit power through a predefined monotonic transmit rate-power function. A rate-adaptive CC mechanism based on the observed channel load is also studied in [11]. In [12], the authors analyzed the distribution of the inter-packet receptions to determine the optimal message transmit parameters. The authors then proposed a joint transmit power/rate control approach for the desired situational awareness range stipulated by upper-layer applications. In this approach, transmit power is determined based on the chosen awareness range, while the BSM scheduling rate is adapted based on the instantaneous channel load. In [13], the authors proposed an awareness centric framework for vehicle safety applications where a joint transmit rate/power control algorithm adapts the awareness quality as a function of the awareness range. The decentralized congestion control (DCC) algorithm, standardized by the European Telecommunications Standards Institute (ETSI) [14], considers the channel load as the feedback input to regulate the message rate. Two approaches have been proposed in [14] – reactive and adaptive. In the reactive approach, depending on the observed load on the channel, the DCC algorithm switches to one of the three possible states: relaxed, active and restrictive. Each of these states has its own transmit rate and power settings. In the adaptive approach, a gate keeping function is defined which allows packets from the upper layers to en-queue in the transmit queue by ensuring that the channel occupancy never exceeds a pre-configured threshold.

2) Medium Access Control (MAC) Based Congestion Control: In [15], the authors proposed a congestion control algorithm that is reinforced by road-side units (RSUs) to improve the communication link quality at road intersections. Typically, suburban or urban intersections are characterized by a non-line of sight (NLOS) environment for around-the-corner

V2V links. Using a $k - means$ algorithm to identify the vehicle clusters in the aggregated intersection vehicle data collected at the RSU, the congestion control unit determines a set of transmit and MAC parameters for each cluster. Determined transmit parameters are then disseminated to the stopped vehicles at the intersection through RSU broadcast. In another work, the authors in [16] took a content-centric MAC scheme to address the V2V scalability issue. The proposed scheme provides a mechanism to adaptively allocate the limited wireless resources to the information objects (V2V entities) based on the number of requests for those. In this approach, the bandwidth of each participating network entity is allocated based on the timeliness and completeness of the information it possesses about a requested region (by other V2V entities). In [17], the authors proposed a distributed CC approach based on a modified CSMA/CA mechanism of the MAC layer that adjusts the contention window size by considering the priority of the user data.

B. Technical Objective

The main focus of this article is the SAE J2945/1 [1] CC algorithm – a joint rate-power adaptation mechanism which is standardized for scalable BSM scheduling protocol based on the measured channel congestion level and the estimated vehicle density. In this algorithm, BSMs are transmitted depending on the vehicle dynamics and the estimated vehicle density in a predetermined radius of the sender vehicle [2], [3]. The algorithm also adapts transmit power as a function of the observed channel load [4]. Using a congestion generation test-bed, [18] demonstrated that the SAE J2945/1 CC protocol can achieve lane-level tracking accuracy under heavy congestion. Recently, [19] validated the effectiveness of the CC algorithm for vehicle mobility extracted from a large-scale field data. Although the results show the efficacy of the algorithm in general, the channel propagation model considered in these studies is calibrated for a controlled open-sky environment. Another work, as reported in [20], investigated the scope for improvement in the congestion control logic.

The first major contribution of this article is to evaluate the SAE J2945/1 CC algorithm using realistic vehicle mobility and channel propagation models. While existing related works evaluate the overall stability and fairness of the algorithm, this article focuses more on the end goal (i.e., tracking accuracy) of the scalable communication among entities in vehicular contexts. To that end, this article presents performance evaluation metrics for cases where reliable communication is most needed. This work includes a significant set of traffic scenarios in the simulation study that covers a variety of representative traffic scenarios. The second major contribution is to further analyze the BSM generation rate and transmit power settings of SAE J2945/1 to reveal any potential room for improvement in the default parameter settings of the algorithm.

C. Paper Organization

The rest of the paper proceeds as follows. Section II provides an overview of the SAE J2945/1 CC algorithm with a brief explanation of its input parameters, and the

BSM rate and transmit power control mechanisms. Section III evaluates the CC algorithm by comparing its performance against a fixed-rate fixed-power baseline scheme to show the algorithm's scalability efficiency in different traffic densities. A comprehensive analysis on the relationship of information dissemination rate with message rate and transmit power is provided in Section IV. Section V provides a trade-off study of the key congestion control parameters that illustrates the resulting safety benefits at different target ranges. And finally, we conclude in Section VI.

II. OVERVIEW OF THE SAE J2945/1 CONGESTION CONTROL ALGORITHM

A feedback-loop based adaptive channel congestion control algorithm is outlined in the SAE J2945/1 which regulates the BSM inter-transmit time and BSM transmit power. A brief overview of this standardized CC mechanism is presented in this section covering the algorithm inputs, BSM scheduling criteria and the transmit power control logic.

A. Algorithm Prerequisites

The SAE J2945/1 BSM scheduling protocol requires a set of input parameters to be updated at a predefined interval to adaptively change the inter-transmit time and transmit power. At every BSM scheduling interval (t_{txCtrl}), the following parameters are considered to make a transmission decision.

- **Vehicle Density (VD):** Each ego-vehicle or host vehicle (HV) keeps track of its surrounding vehicle density by aggregating information from the received BSMs. This quantity is denoted as N_s and essentially computes the number of unique V2V entities within a predefined range (r_{PER}) of the HV. This parameter feeds the CC algorithm with a coarse estimation of the transmitting entities that are contributing to channel congestion.
- **Channel Busy Percentage (CBP):** Expressed as a percentage, this network-level metric measures the proportion of channel occupancy. The channel is declared busy by the radio receiver if a BSM reception is on-going or the energy level is higher than the energy detection threshold. CBP is considered a local feedback measurement available at every V2V node in the network. If t_{busy} is the measured channel busy duration and $t_{cbpIntvl}$ is the period of time over which CBP is being measured, then CBP can be calculated as follows:

$$CBP(\%) = 100 * \frac{t_{busy}}{t_{cbpIntvl}} \quad (1)$$

- **Packet Error Ratio (PER):** This metric essentially quantifies the quality of the communication channel in terms of a time-window based packet loss ratio by determining the number of missed packets at a receiver from a transmitter and the total number of sent packets by that transmitter. The number of the total sent packets is determined from the sequence numbers of received packets.

B. BSM Scheduling

Assuming the time index of each t_{txCtrl} interval is denoted as k , the SAE J2945/1 states that at k -th t_{txCtrl} interval, the host vehicle shall make a BSM transmit decision based on the following criteria:

- If any critical events such as hard-brakes are ongoing, a BSM is scheduled for immediate transmission with the latest vehicle status update.
- Otherwise, perceived tracking error of the HV is estimated by extrapolating its latest position from the last sent BSM considering the channel PER. Depending on the estimated error, a probabilistic BSM transmission due to vehicle dynamics is scheduled as follows:

$$p(k) = \begin{cases} 1 - e^{-\alpha * |err(k) - T|^2}, & \text{if } T \leq err(k) < S \\ 1, & \text{if } err(k) \geq S \\ 0, & \text{Otherwise} \end{cases} \quad (2)$$

where $p(k)$ denotes the transmit probability and $err(k)$ is the estimated tracking error of the host vehicle perceived by the remote vehicles at k -th BSM schedule interval. T and S are the minimum and maximum bounds for tracking errors, respectively.

- Otherwise, an ITT-induced BSM transmission is scheduled based on vehicle density N_s within r_{PER} , as follows:

$$ITT(k) = \begin{cases} 100, & \text{if } N_s(k) \leq \beta \\ 100 * \frac{N_s(k)}{\beta}, & \text{if } \beta < N_s(k) < \frac{itt_{max}}{100} * \beta \\ itt_{max}, & \text{if } \frac{itt_{max}}{100} * \beta \leq N_s(k) \end{cases} \quad (3)$$

where β is the vehicle density coefficient which defines the starting vehicle density to initiate the ITT adaptation of the CC algorithm. The maximum allowed ITT is denoted by an adjustable parameter itt_{max} . The default itt_{max} value is set to 600 milliseconds in the standard based on extensive simulation experiments. The constraint on itt_{max} ensures that the vehicles would disseminate BSMs, even in highly dense traffic conditions, in an attempt to maintain the minimum inter-packet gap as stipulated by safety applications. Since ITT is constrained by itt_{max} , the value chosen for β defines the slope of the ITT change. In eq. 3, N_s is determined from the received BSMs at the HV.

C. Transmit Power Control

Upon making a BSM transmit decision, the SAE J2945/1 compliant V2V radio calculates the corresponding transmit power based on the latest available CBP measurement (referred to as U in the equations below). Eq. 4 determines the raw radiated power which is constrained by U_{min} and U_{max} to keep the offered channel load within the optimal operating range. Radiated power (RP) is then calculated as Eq. 5. And final transmit power is then determined by Eq. 6 by accounting

for the antenna gain G and cable loss $loss_{cable}$.

$$f(U) = \begin{cases} RP_{max}, & \text{if } U \leq U_{min} \\ RP_{max} - \frac{RP_{max} - RP_{min}}{U_{max} - U_{min}} * (U - U_{min}), & \text{if } U_{min} < U < U_{max} \\ RP_{min}, & \text{if } U_{max} \leq U \end{cases} \quad (4)$$

$$RP = RP_{Previous} + SUPRAGain * (f(U) - RP_{Previous}) \quad (5)$$

$$Tx\ Power = RP - G + loss_{cable} \quad (6)$$

For further details regarding the BSM scheduling and transmit power control, an interested reader is referred to [1].

III. EVALUATING THE SAE J2945/1 CONGESTION CONTROL ALGORITHM

Extensive simulations were conducted to evaluate the performance of the SAE J2945/1 CC algorithm in a variety of vehicular environments for different levels of traffic densities. Due to inherently dynamic communication links in vehicular environment, reliable performance evaluation of the CC algorithm in such settings requires an efficient high fidelity simulation platform. In this section, we provide the simulation setup in details and evaluate the performance of the CC algorithm in a variety of representative freeway and intersection scenarios.

A. Simulation Setup

In V2V simulation experiments, capturing realistic vehicle trajectories and wireless propagation behaviors are particularly important for the performance evaluation of any upper layer communication protocols. To that end, we developed a realistic simulation platform using empirical DSRC receiver sensitivity data and large scale received signal strength (RSS) measurement dataset as reported in [21]. We enhanced the ns-3 [22] simulator, a discrete event network simulator, by calibrating various models of the protocol stack using empirical dataset. In the process, RSS dataset from a large-scale field test was obtained to model realistic radio signal propagation in freeway and intersection environments. The RSS measurement campaign collected samples from a carefully chosen freeway region-of-interest on the I-405 in Orange County, CA and from a typical sub-urban 4-way intersection, also located in Orange County, CA. The freeway RSS samples are broadly classified into three different densities based on publicly available loop-sensor data provided by CalTrans PeMS dataset [23]. Relative direction of the sender(Tx)-receiver(Rx) pair is considered in the channel model derivations, as significantly different link quality is observed between the RSS samples from same direction and opposite direction traffic. In the intersection RSS dataset, the path loss appears to have a direct relationship with the relative positioning of the Tx-Rx pair with respect to the center of the intersection. Thus, intersection RSS samples are classified into obstructed-LOS/NLOS and potential-LOS categories. Potential-LOS samples are further categorized into

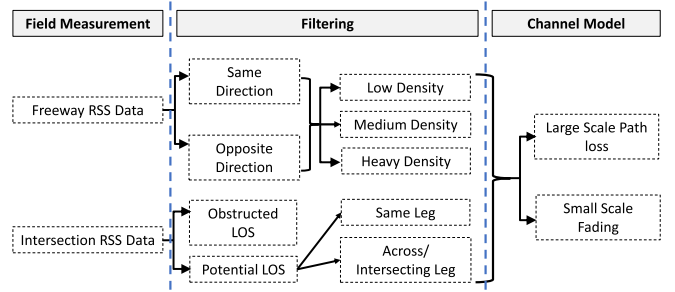


Fig. 1. Classification of the derived channel propagation models based on empirical RSS measurements.

TABLE I
CC ALGORITHM PARAMETER SETTINGS IN SIMULATION

Parameter	Value	Parameter	Value
β	25	itt_{max}	600 ms
RP_{min}	10 dBm	RP_{max}	20 dBm
U_{min}	50%	U_{max}	80%
T	0.2 m	S	0.5 m
α	75	SUPRAGain	0.5
G	0 dB	$loss_{cable}$	0 dB
$t_{txCtrlIntvl}$	100 ms	r_{PER}	100 m

two sets: same-leg and intersecting-leg. In the derivation of channel propagation loss, all Tx-Rx links in freeway (both same and opposite direction) and same-leg intersection scenarios are modeled as a function of 2D Euclidean distance between the Tx-Rx pair. The model for intersecting-leg Tx-Rx link considers the pair's relative distance from the center of the intersection. This distinction was made to further realize the effects of 4-way intersection landscape on channel propagation [24], as vehicle pairs on intersecting road legs typically have an NLOS or partial-LOS. The large-scale path loss component of all these channel models is derived using the two-ray ground reflection model as reported in [25]. The overall flow of the RSS data filtering and the channel propagation modeling procedure is illustrated in Figure 1. For further details on the derivation of the channel models, an interested reader is referred to [26].

In this article, we aim to validate the CC algorithm using the same physical environments where the RSS measurement campaign was conducted. Vehicle mobility traces were also generated for the same traffic environments utilizing a microscopic traffic simulation model. The mobility generation tool is specifically geared to capture the traffic levels at different times of the day. This tool also enabled us to extract the specific vehicle trajectories that match the densities observed during the RSS measurement campaign. A high fidelity DSRC physical layer (PHY) model is used in the simulation experiments, which was validated against a large-scale field dataset as reported in [21] [27]. The CC algorithm settings used in the simulation experiments are tabulated in Table I.

B. Performance Metrics

An evaluation metric called information age (IA), and a performance metric called tracking error (TE) are used in evaluating the performance of the CC algorithm. IA is a useful metric to evaluate the communication performance, while TE

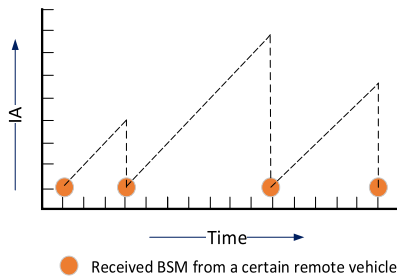


Fig. 2. IA calculation over time. Each tick on both axes represents unit time.

provides more insight into how well a vehicle is eventually tracked using the communicated information. Both IA and TE metrics are calculated from the HV perspective.

1) *Information Age (IA)*: IA, at a given time t , is the lapsed time between t and the timestamp corresponding to the data contained in the latest received information from a particular remote vehicle (RV) and can be expressed as follows.

$$IA_{HV, RV}(t) = t - t_{RV, HV(k_t)} \quad (7)$$

where k_t is the index of the most recent status update received from a RV at the HV until time t and $t_{RV, HV(k_t)}$ is the corresponding message timestamp. Figure 2 illustrates the evolution of IA over time as BSMs from a certain remote vehicle are being received. Typically, received BSMs at the HV (the Rx vehicle) include timestamps of the relevant position status updates of the sender RVs. Therefore, information age starts to grow linearly in time upon a BSM is received from a particular RV until the next BSM is received from that RV. This timestamp is not necessarily the timestamp the BSM is generated by the application layer. Depending on the application settings, a BSM may include coasted GPS position data or actual GPS position data. When GPS data is coasted, the BSM timestamp is the same as the timestamp when the application generates the data. If GPS coasting is disabled, BSM timestamp reflects the actual GPS update time. In our simulations, GPS coasting was enabled.

2) *Tracking Error (TE)*: At a given time t , TE for a particular sender RV is the 2D distance difference between the current position estimate of the sender RV at the HV and the true position of that RV obtained from its GPS log. Since TE sampling is dependent on the availability of actual position updates, the TE metric can be calculated at most at the sampling rate of GPS updates, which is 10 Hz in our simulation experiments. Vehicle dimension and GPS error are not considered in the simulations, and therefore, presented TE results in this article is only affected by the communication link quality and vehicle dynamics. If t is the GPS time at a certain RV and t' is the last received BSM timestamp from that RV at the HV, then the estimated position of the RV at t at the HV can be extrapolated over $\Delta t = t' - t$ using the received BSM information as follows:

$$\begin{cases} \hat{x} = \tilde{x} + \Delta t * \tilde{v} * \cos(\tilde{\theta}) \\ \hat{y} = \tilde{y} + \Delta t * \tilde{v} * \sin(\tilde{\theta}) \end{cases} \quad (8)$$

where (\hat{x}, \hat{y}) is the current position estimate of the RV at the HV, assuming Cartesian coordinate system and constant



Fig. 3. Highlighted stretch of the I-405 Freeway in Orange County, CA is chosen as the region of interest for freeway RSS measurement, and for validating the CC algorithm. Source: Google Inc ©.

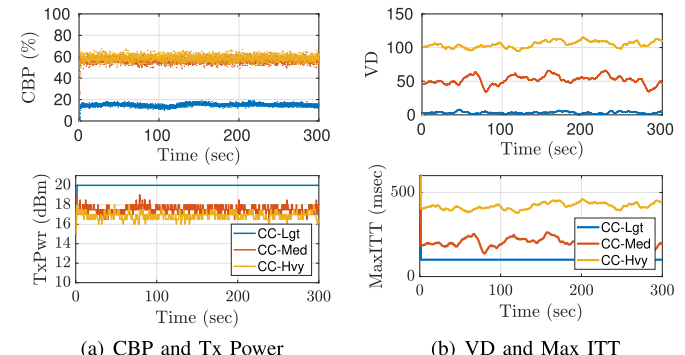


Fig. 4. CBP, Transmit Power, Vehicle Density (VD) within 100 m radius and Max ITT for different traffic density cases.

velocity model, and (\tilde{x}, \tilde{y}) is the latest received BSM position from the RV with a speed value of \tilde{v} . The tracking error TE can then be calculated as follows:

$$TE_{HV, RV}(t) = d((\hat{x}, \hat{y}), (x, y)) \quad (9)$$

where $d(., .)$ is the 2D Euclidean distance, in meters.

C. Evaluating CC Algorithm in Freeway Scenarios

To evaluate the performance of the CC algorithm in freeway scenarios, we selected a 3.5-kilometer section of the I-405 freeway in Orange County, CA, which is stretched between the I-405/I-605/SR-22 and I-405/SR-22 junctions (Figure 3). The selected stretch of the freeway consists of 8 lanes (including two High Occupancy Vehicle lanes) in each direction. Realistic vehicle mobility traces are generated using a calibrated micro-simulation mobility tool. The mobility generation tool also enabled us to accurately timestamp the hard-braking events as well as the lane-change maneuvers. The simulated vehicular environments are broadly categorized into light, medium and heavy traffic scenarios where the vehicle densities of these categories are 10, 25 and 50 vehicles/mile/lane, respectively.

To begin the evaluation, we first seek to verify that the supporting metrics (CBP, MaxITT) calculated from the simulation results from a subject vehicle are in line with the expected behavior of the CC algorithm. Figure 4(a) shows the CBP and transmit power measured at the subject vehicle. It suggests that the transmit power is adjusted adaptively based on the measured channel load. And thus, channel load is kept within the optimal operating range. Figure 4(b) shows how the ITT is adaptively adjusted based on the calculated vehicle density, to regulate the offered load to the channel.

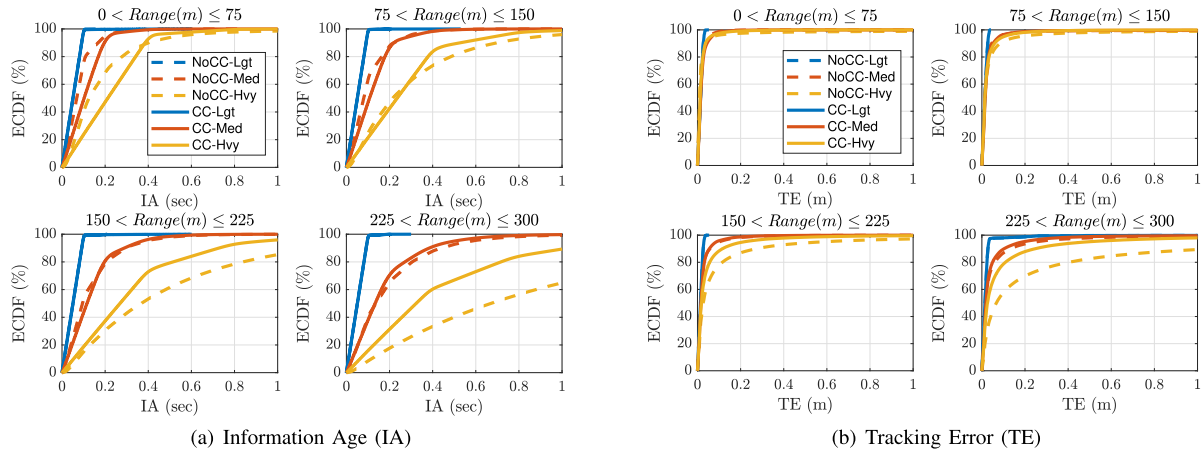


Fig. 5. Performance evaluation of NoCC vs. CC in freeway scenarios. Empirical CDFs are calculated for samples pertaining to same direction traffic. The samples are aggregated regardless of the remote vehicle maneuvers.

Figure 5 shows the IA and TE comparisons of the baseline (NoCC) and CC algorithm in terms of empirical cumulative distribution function (ECDF). IA for light and medium densities are similar for both the baseline and CC algorithm. When the channel is loaded below the optimal level, the baseline is expected to achieve similar performance as the CC algorithm. When the channel gets congested with BSMs from an increased number of transmitting vehicles, as is the case for the heavy traffic scenario we simulated, IA of the CC algorithm outperforms the IA of NoCC. The disparity in the IA performance of CC and NoCC is more evident at farther ranges. Higher traffic density translates to a higher number of BSM transmissions which essentially increases the probability of over-the-air packet collision. As a result, BSMs from farther ranges have a greater loss ratio compared to the BSMs from closer ranges. The reason is that the BSMs from farther distances will attenuate more, resulting in a relatively lower received power at the HV side. In general, the CC algorithm keeps the interference level at a minimal by reducing the BSM transmit rate as density increases. Additionally, it adapts transmit power to limit the interference range. The rate and power adaptation jointly results in relatively lower IA for the CC algorithm at farther ranges (but still within desired awareness range).

The TE metric depends on the corresponding IA and vehicle dynamics. Figure 5(b) shows how tracking accuracy of the CC algorithm compares with baseline. It is observed that, while both the baseline transmit protocol and the CC algorithm perform well on tracking accuracy, the CC algorithm achieves slightly better accuracy. The performance gain once again has a wider margin at farther ranges. It is important to note that by design the CC algorithm allows the ITT to grow to some extent as long as it is not violating the criteria for tracking-error induced transmission. This aspect of the algorithm helps improving the performance at farther ranges while still keeping the safety requirements in check for nearby vehicles. In contrast, the NoCC approach keeps transmitting BSMs at a flat 10Hz rate, and trades off the performance of farther ranges in favor of closer ranges. Therefore, in some cases, the NoCC

performance at closer ranges might seem slightly better when compared to CC performance, albeit the performance gap is very narrow. At farther ranges, the CC performance significantly outperforms NoCC in all cases. The performance gain of CC algorithm becomes more obvious in heavier density scenarios as shown in Table II, which includes the following two scenarios: a scenario that resembles a backed-up traffic on one side of the freeway (121 veh/mile/lane) while the other side is relatively free-flowing (36 veh/mile/lane); and another scenario where both sides of the freeway are backed-up (one side with 121 veh/mile/lane and the other side with 113 veh/mile/lane).

As mentioned in Section II, the CC algorithm transmits event-driven and dynamics-driven BSMs to further the situational awareness. It is important to note that most of the exchanged BSMs in a given vehicular scenario are due to ITT-induced transmissions which are essentially guard BSMs. Therefore, a lower generation rate for the ITT-induced transmissions ensures that the critical BSMs, i.e., event-driven and vehicle dynamics-driven BSMs can get through in a timely manner. Event-driven BSMs are transmitted when the hard-brake is applied, i.e., when the vehicle decelerates at a higher rate. Vehicle dynamics driven BSMs are typically transmitted during quick vehicle maneuvers and are generally triggered during lane changes. The microscopic traffic simulation tool we used to generate realistic vehicle trajectories enabled us to timestamp the span of critical events and lane-change maneuvers for each vehicle. Using that information we can filter the IA and TE samples by critical event and lane-change maneuvers. The tracking performance of the CC algorithm during lane-change and critical event conditions, as shown in Figure 6, outperforms the NoCC transmit approach. This substantial gain in tracking accuracy can be attributed to the lower interference levels the critical BSMs experience. Typically, at a given time a small subset of the total participating transmitting nodes engage in hard-braking or lane-changing maneuvers. Therefore, the inter-transmit times of this subset go low, while the rest of the vehicles communicate at higher intervals (guard intervals). The net interference level,

TABLE II
90-TH PERCENTILE IA AND TE FOR ONE-SIDE AND BOTH-SIDE BACKED-UP FREEWAY SCENARIOS

Traffic Density	Range	NoCC IA (s)	CC IA (s)	NoCC TE (m)	CC TE (m)
One-side blocked (78veh/mile/lane)	0m - 75m	0.824	0.570	0.099	0.075
	75m - 150m	1.833	0.922	0.427	0.131
	150m - 225m	3.498	1.339	1.273	0.246
Both-side blocked (117veh/mile/lane)	0m - 75m	1.687	0.815	0.159	0.063
	75m - 150m	4.553	1.415	0.780	0.121
	150m - 225m	9.075	2.543	2.004	0.480

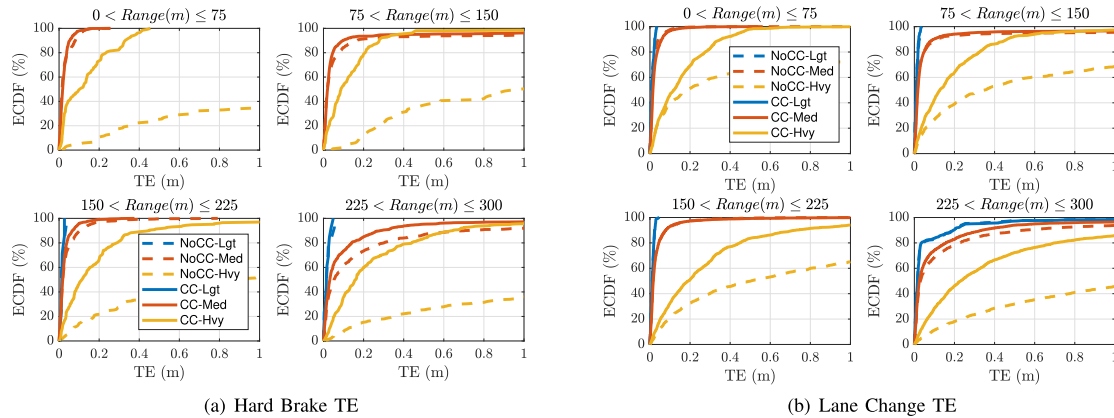


Fig. 6. Tracking errors during hard-braking and lane change maneuvers of remote vehicles.

TABLE III

90-TH PERCENTILE IA AND TE FOR INTERSECTION SCENARIOS – RESULTS ARE FILTERED BASED ON RELATIVE POSITIONS OF THE SENDER-RECEIVER PAIRS ON THE SAME ROAD AND INTERSECTING ROADS

Density	Road Type	Range	NoCC IA (s)	CC IA (s)	NoCC TE (m)	CC TE (m)
Light (< 20veh/mile/lane)	Same	0m - 50m	0.092	0.131	0.013	0.015
		50m - 100m	0.096	0.157	0.020	0.021
		100m - 150m	0.150	0.187	0.028	0.044
	Intersecting	0m - 50m	0.094	0.135	0.009	0.010
		50m - 100m	0.153	0.218	0.011	0.014
		100m - 150m	0.298	0.365	0.087	0.083
Heavy (> 20veh/mile/lane)	Same	0m - 50m	0.218	0.459	0.020	0.064
		50m - 100m	0.445	0.513	0.134	0.184
		100m - 150m	0.929	0.848	0.313	0.276
	Intersecting	0m - 50m	0.253	0.420	0.041	0.139
		50m - 100m	0.758	0.643	0.217	0.206
		100m - 150m	1.775	0.854	3.243	0.589

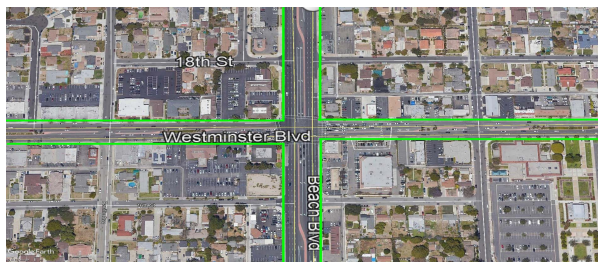


Fig. 7. 4-way Intersection of Beach Boulevard and Westminster Avenue in Orange County, CA. Source: Google Inc ©.

therefore, for the time-critical BSMs is low, and that leads to a higher successful receive ratio and eventually, higher tracking accuracy.

D. Evaluating CC Algorithm in Intersection Scenarios

To evaluate the performance of the CC algorithm in intersection scenarios, the intersection of Beach Boulevard and Westminster Avenue in Orange County, CA is selected (illustrated in Figure 7). This is a typical 4-way signalized suburban

intersection and characterized by building blocks on each corner, effectively creating a NLOS/partial-LOS condition for the communicating vehicle pairs on perpendicular roads. Vehicles on the same-leg or same-road generally have LOS conditions, ignoring the blockage created by in-between vehicle bodies. Due to diverse communication link characteristics in such intersection scenarios, we look into performance measures by filtering the IA and TE samples based on the relative position of the Tx-Rx pair. Two different road leg types are considered in this way: *same-road* is denoted to samples when Tx-Rx pair are on the same road having a potential-LOS and *intersecting-road* to samples when Tx-Rx pair are on intersecting road legs with NLOS or partial-LOS. We also bounded our region of interest (ROI) to a 100m range from the center of the intersection, as most of the vehicles in this environment are concentrated around the intersection. The ROI-filtered samples are then binned based on the 2D distance of corresponding Tx-Rx links. Table III captures the IA and TE measures for CC and NoCC cases. Note that the range bin size and maximum range for intersection results are different than the results shown in freeway scenarios. Vehicle densities in intersection

scenarios are relatively low compared to freeways, and from the safety application perspective, 150 meters is thus deemed to be sufficient in such environments. From Table III, we make the following observation: while the baseline performance is slightly better at closer ranges, the obvious benefits of CC are noticeable at farther ranges. Note that the CC algorithm, by design, allows the perceived tracking error to grow to some extent (eq. 2) by increasing the inter-transmit time. This mechanism helps reduce the interference level at the intended receivers and enables BSMs from farther ranges to be received.

IV. OPTIMIZING INFORMATION DISSEMINATION RATE

In this section, we seek to establish the adequacy of the default parameter settings of the SAE J2945/1 CC algorithm. In the process, we consider the effect of the realistic channel propagation models we used in the simulation experiments discussed above. Since, from the cooperative vehicle communication viewpoint, maximizing the amount of delivered information to the neighboring vehicles is a desired feature, we look into the performance measure referred to as Information Dissemination Rate (IDR) in [3]. In vehicular communication context, the IDR metric is an indicator of how well neighboring vehicles can communicate with each other and quantifies the number of successfully received BSMs by a set of receiving vehicles from a certain transmitter. Typically, V2V applications tend to track a small subset of the vehicles in close proximity, and therefore, IDR measurements at a set of target safety ranges are more meaningful than IDRs measured over the entire communication range. If there are N nodes within the range of interest of a transmitter, IDR can be calculated as follows.

$$IDR = \sum_{i=N/2}^{N/2} SRR(i) \quad (10)$$

where $SRR(\cdot)$ is the successful reception rate at the receivers within the range of the subject transmitter.

Since all the transmitting nodes use CSMA/CA mechanism for medium access, and assuming similar hidden nodes situation for all nodes in a homogeneous traffic density scenario, IDR is expected to be similar for all nodes. Thus, IDR can be calculated from the receiving node's perspective as well. Hence, the quantity in Eq. 10 equates to the number of successfully received messages by a receiving vehicle in per unit time, from all the transmitting vehicles within the range of interest. In DSRC, participating vehicles employ a broadcast transmit mode which does not have any handshake protocol in place. Therefore, the energy detection threshold (EDT) of the V2V radio devices may become a determining factor of IDR. Typically, EDT is not configurable at run-time, and is mostly implementation dependent. Furthermore, IDR can be defined over the entire communication range as well as over a range of interest. From vehicle safety perspective, IDR needs to be maximized over an application-specific critical range rather than the entire communication range. As a result, the impact of transmit rate and power is required to be analyzed for designing optimal channel congestion management schemes. IDR is an application-layer level metric and depends on the

choices of rate and transmit power, and thus, has the following relationship:

$$IDR \stackrel{\text{def}}{=} h(R, P) \quad (11)$$

where R is the set of rate values and P is the set of transmit power values. The end goal of the CC algorithm is to find the optimal combination of these parameters that maximizes the IDR. Thus, we can formulate the objective function of the CC algorithm as follows:

$$\begin{aligned} & \underset{R, P}{\text{maximize}} \quad IDR \\ & \text{subject to } R_{min} \leq R \leq R_{max}, \quad P_{min} \leq P \leq P_{max}. \end{aligned} \quad (12)$$

where message rate R is bounded between R_{min} and R_{max} , and transmit power P is bounded between P_{min} and P_{max} .

A. Simulation Study on IDR

In the next subsection, we analyze different aspects of the IDR metric by setting up a simulation environment with a hypothetical 8-kilometer long 1-D roadway. Transmitting nodes are placed with uniform spacing in-between. In the experiments, we vary node density ρ to determine the impact of PHY and MAC layers on IDR. Channel load U for a given density is varied by varying the message generation rate R and the transmit power P . We set EDT to -82 dBm as found by the hardware test reported in [6]. Furthermore, we use the channel propagation model derived for heavy traffic conditions in the freeway scenario, as mentioned in Section III.

B. BSM Rate, Transmit Power and IDR

To determine how BSM rate (inter-transmit interval), transmit power and IDR are related, we perform simulations for different rate and power settings for varying node density levels. Figure 8 shows that a higher BSM rate generally achieves higher IDR when vehicle density is lower. As vehicle density increases, maximum IDRs tend to be achieved at lower message rates. Another observation we made is that for a given density, a lower message rate achieves higher IDRs at higher ranges. This observation can be explained using the interference characteristics of transmitting nodes. Handshake RTS/CTS mechanism is not available in CSMA/CA based cooperative vehicle communication systems as such networks use broadcast transmit protocol. All contending nodes, therefore, use the same contention window (CW) (assuming similar IP traffic with same user priority) for channel access which potentially increases the possibility of multiple nodes count down to zero after their respective back-off procedures. This allows packets from multiple transmitting nodes to collide concurrently. This is very commonplace for V2V communication as smaller contention window is preferable due to the latency requirements set forth by V2V safety applications. Furthermore, the transmitting nodes involved in concurrent packet collisions are usually closely located to the origin of the signal of interest (SOI), which results in a lower signal-to-interference-and-noise-ratio (SINR) for the SOI at the receiver end. SOI is essentially the signal corresponding to the packet the receivers are trying to receive. Another factor affecting

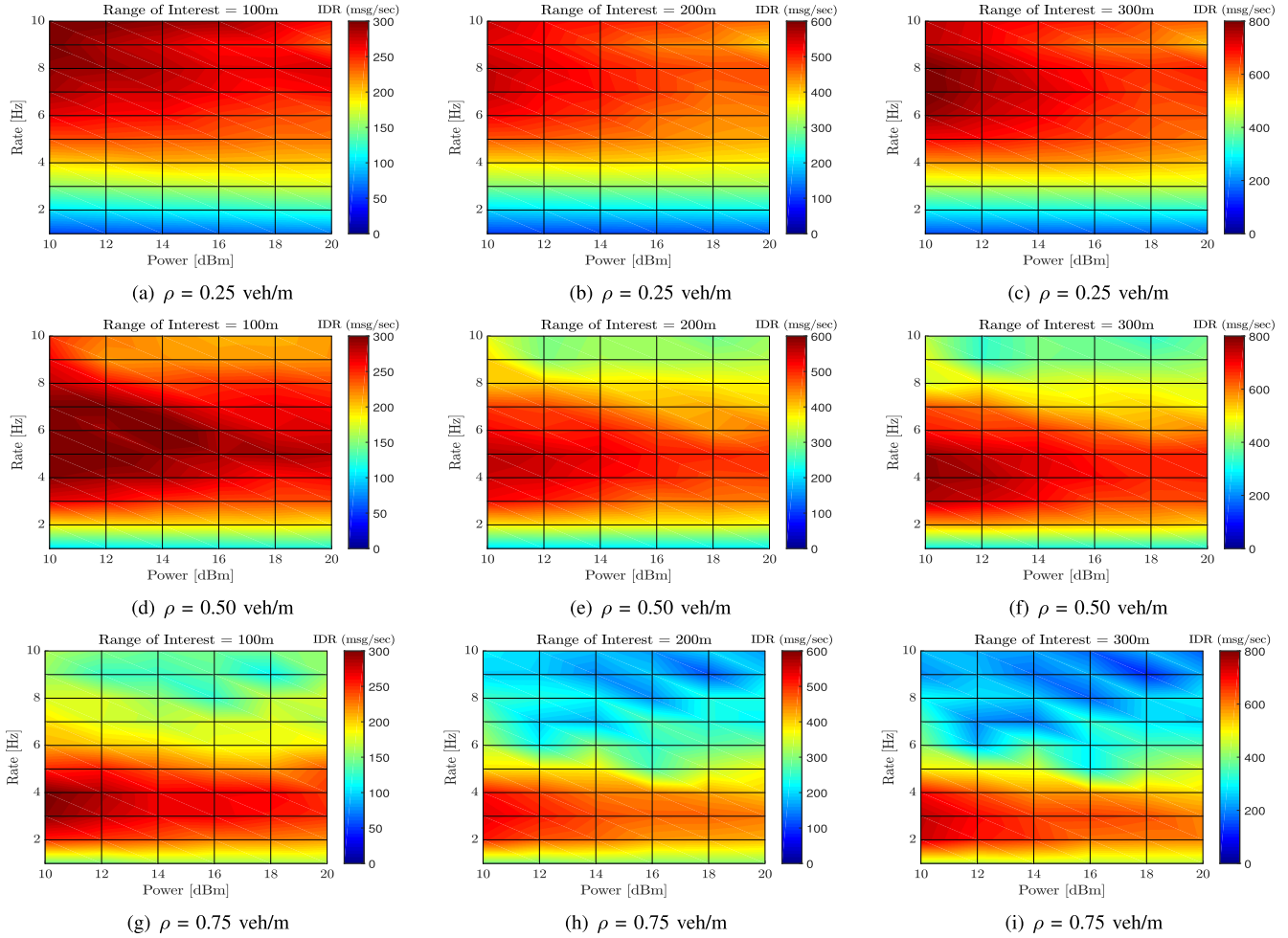


Fig. 8. IDR vs. Message Rate and Transmit Power (EDT = -82 dBm).

the packet collision rate is the presence of hidden nodes. This phenomenon particularly affects V2V communication due to its high fading and high shadowing channels. Typically, nodes that are geographically far apart tend to appear as hidden nodes to each other. The spatial relationship between the SOI and interference signals can explain the IDR gain at lower message rates in a congested scenario. Here, SOI is the incoming signal that the receiver is eventually tuned to for reception after preamble detection and frame capture (if any). When the last bit of the SOI arrives at the receiver antenna, it decides whether the total frame can be declared successfully decoded. In our simulator, this decode decision is made using an empirical error rate model which is a function of SINR of the SOI [6]. Figure 9 graphs the distances of the interferer nodes to the RX vehicle that are deemed hidden to each other. It also shows the distances of interfering nodes that count down to zero at the same time as the SOI node, to gain access to the channel. Note that we graph only the positions of the interfering nodes the signals from which are above the noise floor (-98 dBm). In this article, packet collisions due to multiple nodes being reached to the end of the back-off timer are referred to as the *concurrent collision*. Figure 9 shows that when BSM transmit interval is sparse (BSM Rate = 2 Hz), the number of concurrent collisions and collisions due to

hidden nodes are significantly low. An increase in the BSM rate (10 Hz) also increases the packet collisions of both kinds. Increased concurrent collisions are particularly detrimental for successful packet reception, as transmitting nodes contributing to concurrent collisions are geographically located at close proximity of each other and the SOI node, and therefore, severely impact the SINR level of SOI. In contrast, distances between the SOI and hidden nodes are usually greater, which naturally have a lower impact on the SINR of SOI. The rate control component of the CC algorithm helps reduce the concurrent collisions significantly, which essentially benefits the upper layer performance metrics in dense traffic conditions. With a lower number of overall BSMs being exchanged by the CC algorithm, the number of hidden node collisions is also get reduced.

C. Channel Occupancy and IDR

Figure 10 shows the IDR measures for different channel occupancy levels for varying vehicle densities of 0.25, 0.50 and 0.75 veh/m, with different transmit powers used for the BSMs. Noting the channel occupancy levels corresponding to the maximum achievable IDR, we see that for an under-utilized or saturated channel, the CBP values associated

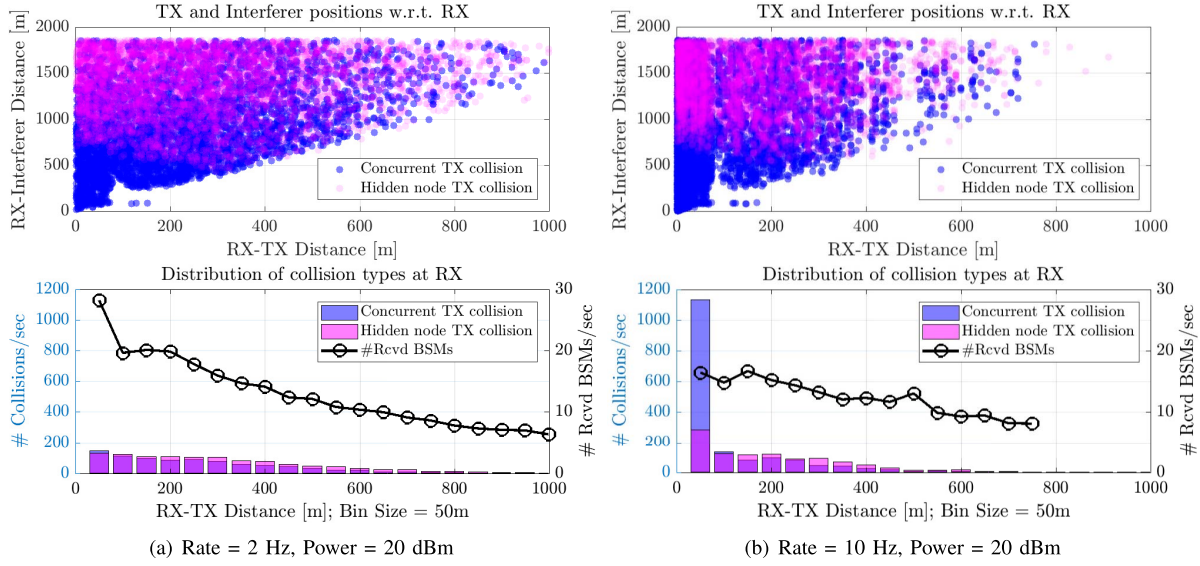


Fig. 9. Packet collision statistics of all the received packets (from all neighbors in communication range) at the subject vehicle for vehicle density of 0.75 veh/m. Distance of SOI node and interfering nodes are calculated with respect to the receiver node. The right Y-axis shows the number of received BSMs per second at the receiver from different ranges.

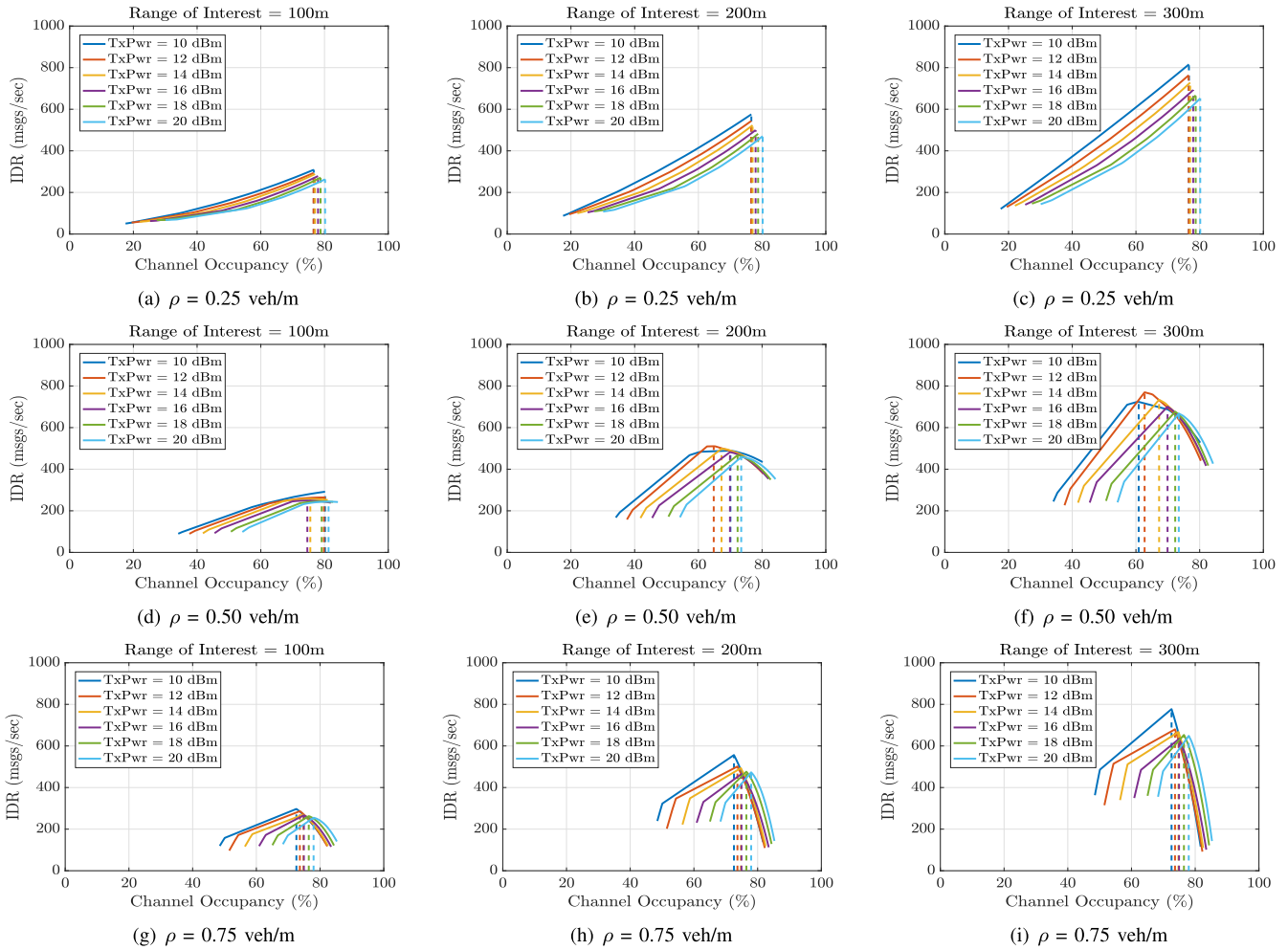
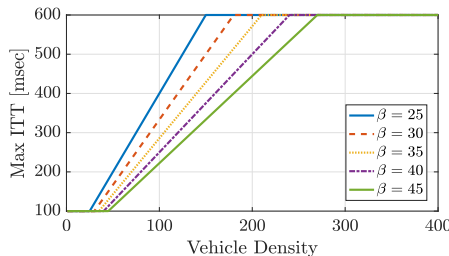


Fig. 10. IDR versus Channel Occupancy for different TxPower levels. The vertical lines correspond to the maximum of each of the TxPower-IDR curves.

with optimal IDR values remain similar for individual power levels at different ranges. It is also observed that the optimal CBP

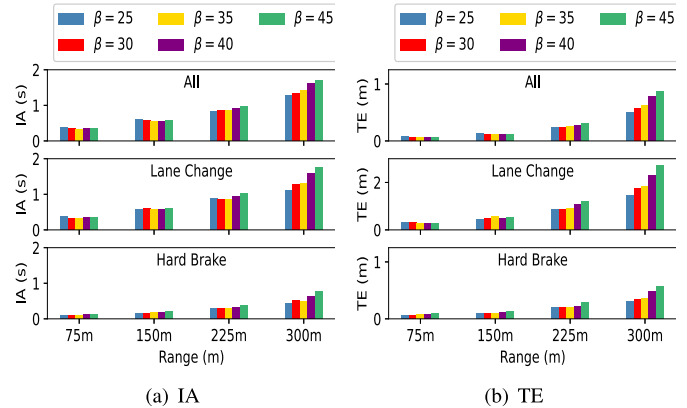
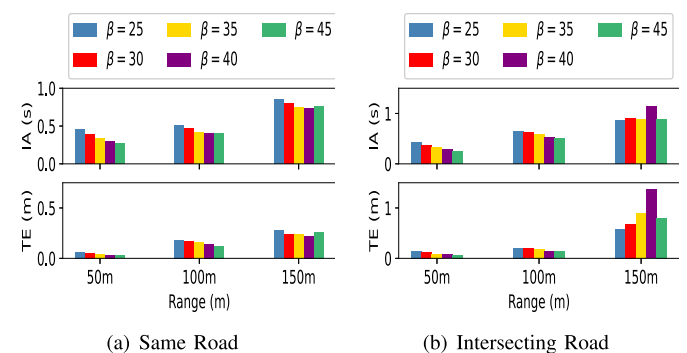
varies for different IDR ranges of interest, but generally remains within 60%-80%, which suggests that the current

Fig. 11. Max ITT for different density coefficients (β).

settings of the minimum and maximum channel utilization in the CC algorithm are in good agreement with realistic traffic environments which are realized using the propagation models derived from field RSS dataset. Currently, the minimum and maximum channel utilization parameters in SAE J2945/1 CC algorithm are set to 50% and 80%, respectively.

V. OPTIMIZING SAE J2945/1 CONGESTION CONTROL PARAMETERS

From the simulation experiments using mobility traces obtained from calibrated microscopic traffic simulation tool, we observe that the frequency of BSM transmissions due to higher-order vehicle dynamics or hard-braking events are relatively lower compared to the ITT-induced (guard interval triggered) BSM transmissions. Therefore, most of the channel load is offered by the density-dependent ITT-induced BSMs as defined in (3). In the CC algorithm, the default value of itt_{max} is to 600 milliseconds (~ 1.67 Hz). However, based on extensive simulation results for different channel conditions, it is observed that the BSM generation rate of 2-3 Hz yields optimal IDR in a highly congested scenario (Figure 8). This observation may call for a further tuning of the rate control component in the CC algorithm. One potential parameter change could be setting itt_{max} to the optimal BSM rate value observed in the simulation study. However, doing so will limit the flexibility of accommodating an increasing number of nodes. Therefore, a more favorable improvement option would be to adjust the slope of ITT as defined in (3) which defines how the ITT changes over different density values considering the configured vehicle density coefficient (β) value. A lower β value means a more aggressive ITT changes as the density changes. Figure 11 shows the ITT changes for different β values. We carried out simulations for a range of β values to see how the tracking accuracy compares over different distance ranges of interest. From Figure 12 and Figure 13, we observe that a higher density coefficient sacrifices some of the tracking gains at higher ranges while affording a better tracking accuracy at closer ranges. Based on these observations and given the generally lower tracking errors observed at closer distances, we can conclude that the current β setting of SAE J2945/1 CC algorithm works acceptably in terms of safety benefits, albeit with some small room for improvement. The study of β variation is done to complete the investigation of finding room for significant improvement in the SAE J2945/1 congestion control algorithm.

Fig. 12. 90-th Percentile IA and TE for different β values in freeway scenarios with Heavy traffic.Fig. 13. 90-th Percentile IA and TE for different β values in intersection scenarios.

VI. CONCLUDING REMARKS

We evaluated the SAE J2945/1 congestion control algorithm by presenting extensive simulation experiments using realistic vehicle trajectories. The validation process used a large-scale field RSS dataset to derive realistic channel propagation models. Vehicle mobility traces were also generated utilizing a microscopic traffic simulation model for the same traffic environments where the field RSS measurement was conducted. Presented results show that the congestion control algorithm achieves significant performance gain in terms of information age and tracking accuracy in dense traffic scenarios. Further analysis of the relationship of message rate and transmit power with the information dissemination rate reveals a potential area of improvement to optimize the vehicle density coefficient parameter of the congestion control algorithm. Simulation experiments were performed to find an optimal value for this parameter and results indicate that the choices of this parameter value come with a trade-off of safety benefits at different ranges of interest. A less aggressive rate control approach with a higher density coefficient achieves slightly better tracking gain at closer ranges, trading off greater safety benefits at farther distances.

ACKNOWLEDGMENT

This work was partly done during an internship at General Motors Global Research and Development Center, Warren, MI, USA.

REFERENCES

- [1] *Surface Vehicle Standard On-Board System Requirements for V2V Safety Communications, J2945/1*, SAE Int., Warrendale, PA, USA, Mar. 2016.
- [2] C.-L. Huang, Y. Fallah, R. Sengupta, and H. Krishnan, "Adaptive intervehicle communication control for cooperative safety systems," *IEEE Netw.*, vol. 24, no. 1, pp. 6–13, Jan. 2010.
- [3] Y. P. Fallah, C.-L. Huang, R. Sengupta, and H. Krishnan, "Analysis of information dissemination in vehicular ad-hoc networks with application to cooperative vehicle safety systems," *IEEE Trans. Veh. Technol.*, vol. 60, no. 1, pp. 233–247, Jan. 2011.
- [4] Y. P. Fallah, N. Nasiriani, and H. Krishnan, "Stable and fair power control in vehicle safety networks," *IEEE Trans. Veh. Technol.*, vol. 65, no. 3, pp. 1662–1675, Mar. 2016.
- [5] *IEEE Standard for Information Technology—Telecommunications and Information Exchange Between Systems Local and Metropolitan Area Networks—Specific Requirements Part 11 Wireless LAN Medium Access Control (MAC) and Physical Layer (PHY) Specifications*, IEEE Standard 802.11-2012 (Revision IEEE Std 802.11-2007), Mar. 2012, pp. 1–2793.
- [6] "Interoperability issues of vehicle-to-vehicle based safety system project (V2V-interoperability) phase 2 final report volume 1—Communications scalability for V2V safety development," NHTSA Publication, Tech. Rep. USDOT NHTSA-2015-0060-0001, 2015, vol. 1, pp. 1–106.
- [7] S. A. A. Shah, E. Ahmed, F. Xia, A. Karim, M. Shiraz, and R. M. Noor, "Adaptive beaconing approaches for vehicular ad hoc networks: A survey," *IEEE Syst. J.*, vol. 12, no. 2, pp. 1263–1277, Jun. 2018.
- [8] J. T. Willis, A. Jaekel, and I. Saini, "Decentralized congestion control algorithm for vehicular networks using oscillating transmission power," in *Proc. Wireless Telecommun. Symp. (WTS)*, Apr. 2017, pp. 1–5.
- [9] G. Bansal, J. B. Kenney, and C. E. Rohrs, "LIMERIC: A linear adaptive message rate algorithm for DSRC congestion control," *IEEE Trans. Veh. Technol.*, vol. 62, no. 9, pp. 4182–4197, Nov. 2013.
- [10] H. Lu, G. Bansal, and J. Kenney, "A joint rate-power control algorithm for vehicular safety communications," in *Proc. ITS World Congr.*, 2015, pp. 1–12.
- [11] A. Weinfield, J. Kenney, and G. Bansal, "An adaptive DSRC message transmission interval control algorithm," in *Proc. ITS World Congr.*, Oct. 2011, pp. 1–12.
- [12] M. Torrent-Moreno, J. Mittag, P. Santi, and H. Hartenstein, "Vehicle-to-vehicle communication: Fair transmit power control for safety-critical information," *IEEE Trans. Veh. Technol.*, vol. 58, no. 7, pp. 3684–3703, Sep. 2009.
- [13] B. Kloiber, J. Harri, T. Strang, S. Sand, and C. R. Garcia, "Random transmit power control for DSRC and its application to cooperative safety," *IEEE Trans. Dependable Secure Comput.*, vol. 13, no. 1, pp. 18–31, Jan. 2016.
- [14] *Intelligent Transport Systems (ITS); Decentralized Congestion Control Mechanisms for Intelligent Transport Systems operating in the 5 GHz range; Access layer part*, document ETSI TC ITS, Technical Specification 102 687 1.2.1, Apr. 2018.
- [15] N. Taherkhani and S. Pierre, "Centralized and localized data congestion control strategy for vehicular ad hoc networks using a machine learning clustering algorithm," *IEEE Trans. Intell. Transp. Syst.*, vol. 17, no. 11, pp. 3275–3285, Nov. 2016.
- [16] S. Kumar, L. Shi, N. Ahmed, S. Gil, D. Katabi, and D. Rus, "Carspeak: A content-centric network for autonomous driving," in *Proc. ACM SIGCOMM Conf. Appl., Technol., Archit., Protocols Comput. Commun.*, 2012, pp. 259–270.
- [17] X. Shen, X. Cheng, R. Zhang, B. Jiao, and Y. Yang, "Distributed congestion control approaches for the IEEE 802.11p vehicular networks," *IEEE Intell. Transp. Syst. Mag.*, vol. 5, no. 4, pp. 50–61, Winter 2013.
- [18] S. A. Ahmad, A. Hajisami, H. Krishnan, F. Ahmed-Zaid, and E. Moradi-Pari, "V2 V system congestion control validation and performance," *IEEE Trans. Veh. Technol.*, vol. 68, no. 3, pp. 2102–2110, Mar. 2019.
- [19] A. Rostami, H. Krishnan, and M. Gruteser, "V2V safety communication scalability based on the SAE j2945/1 standard," in *Proc. ITS Amer. Annu. Meeting*, 2018, pp. 1–10.
- [20] S. Lim and H. Kim, "Improving information age in SAE J2945 congestion-controlled beaconing," *IEEE Commun. Lett.*, vol. 23, no. 2, pp. 358–361, Feb. 2019.
- [21] S. M. O. Gani, A. Tahmasbi-Sarvestani, M. Fanaei, and Y. P. Fallah, "High fidelity DSRC receiver model for NS-3 simulation using large-scale field data," in *Proc. IEEE Wireless Commun. Netw. Conf.*, Apr. 2016, pp. 1–6.
- [22] (2018). *The NS-3 Network Simulator*. [Online]. Available: <http://www.nsnam.org>
- [23] *Caltrans Performance Measurement System*. Accessed: Sep. 10, 2018. [Online]. Available: <http://pems.dot.ca.gov/>
- [24] S. M. O. Gani, Y. P. Fallah, and S. A. Ahmad, "Identifying DSRC channel loss factors of urban intersections using RSS datasets," in *Proc. IEEE 88th Veh. Technol. Conf.*, Aug. 2018, pp. 1–7.
- [25] C. Sommer, S. Joerer, and F. Dressler, "On the applicability of two-ray path loss models for vehicular network simulation," in *Proc. IEEE Veh. Netw. Conf. (VNC)*, Nov. 2012, pp. 64–69.
- [26] E. E. Marvasti, S. M. O. Gani, and Y. P. Fallah, "A statistical approach toward channel modeling with application to large scale censored data," *IEEE Trans. Intell. Transp. Syst.*, to be published.
- [27] Y. P. Fallah and S. M. O. Gani, *Efficient and High Fidelity DSRC Simulation*. Cham, Switzerland: Springer, 2019, pp. 217–243.



S M Osman Gani (Member, IEEE) received the B.S. degree from the Bangladesh University of Engineering and Technology, Dhaka, Bangladesh, the M.S. degree from West Virginia University, Morgantown, WV, USA, in 2015, and the Ph.D. degree from the University of Central Florida, Orlando, FL, USA, in 2019. His current research interests include automated and connected vehicle safety systems and intelligent transportation systems.



Yaser P. Fallah received the Ph.D. degree from The University of British Columbia, Vancouver, BC, Canada, in 2007. From 2011 to 2016, he was an Assistant Professor with West Virginia University (WVU), Morgantown, WV, USA. Prior to joining WVU, from 2008 to 2011, he was a Research Scientist with the Institute of Transportation Studies, University of California at Berkeley. Since 2016, he has been an Associate Professor with the Department of Electrical and Computer Engineering, University of Central Florida, Orlando, FL, USA. His current research interests, sponsored by industry and USDOT and NSF awards, include intelligent transportation systems and involves analysis and design of automated and connected vehicle safety systems. He was the Chair of the IEEE Connected and Automated Vehicles Symposium in 2018, 2019, and 2020. He is an Editor of the IEEE TRANSACTIONS ON VEHICULAR TECHNOLOGY.



Hariharan Krishnan received the Ph.D. degree from the University of Michigan, Ann Arbor, MI, USA, in 1992. He was a Visiting Assistant Research Engineer with the California PATH, University of California at Berkeley, Berkeley, from June 1999 to June 2000. He is a Technical Fellow in the areas of connected and automated vehicles with the Electrical and Controls Systems Research Laboratory, GM Global Research and Development Center. Prior to joining GM in 2001, he was an Assistant Professor with the National University of Singapore, Singapore, from January 1993 to December 2000. He was awarded the prestigious U.S. Government Award for Safety Engineering in 2015. He received the SAE Arch T. Colwell Merit Award in 2013, the SAE Vincent Bendix Automotive Electronics Engineering Award in 2013, and the SAE ITS Award, Outstanding Long-Term Accomplishments to ITS in 2011.